



Sedimentary molybdenum cycling in the aftermath of seawater inflow to the intermittently euxinic Gotland Deep, Central Baltic Sea



Florian Scholz^{a,*}, Matthias Baum^a, Christopher Siebert^a, Sümeyya Eroglu^a, Andrew W. Dale^a, Michael Naumann^b, Stefan Sommer^a

^a GEOMAR Helmholtz Centre for Ocean Research Kiel, Wischhofstraße 1-3, 24148 Kiel, Germany

^b Leibniz Institute for Baltic Sea Research Warnemünde, Seestraße 15, 18119 Rostock, Germany

ARTICLE INFO

Editor: Michael E. Böttcher

Keywords:

Molybdenum isotopes
Manganese
Early diagenesis
Baltic Sea
Paleo-redox

ABSTRACT

Molybdenum (Mo) concentrations and isotope compositions in sediments and shales are commonly used as proxies for anoxic and sulfidic (i.e., euxinic) conditions in the water column of paleo-marine systems. A basic assumption underlying this practice is that the proxy signal extracted from the geological record is controlled by long-term (order of decades to millennia) Mo scavenging in the euxinic water column rather than Mo deposition during brief episodes or events (order of weeks to months). To test whether this assumption is viable we studied the biogeochemical cycling of Mo and its isotopes in sediments of the intermittently euxinic Gotland Deep in the central Baltic Sea. Here, multiannual to decadal periods of euxinia are occasionally interrupted by inflow events during which well-oxygenated water from the North Sea penetrates into the basin. During these events manganese (Mn) (oxyhydr)oxide minerals are precipitated in the water column, which are known to scavenge Mo. We present sediment and pore water Mo and Mo isotope data for sediment cores which were taken before and after a series of inflow events between 2014 and 2016. After seawater inflow, pore water Mo concentrations in anoxic surface sediments exceed the salinity-normalized concentration by more than two orders of magnitude and coincide with transient peaks of dissolved Mn. A fraction of the Mo liberated into the pore water is transported by diffusion in a downward direction and sequestered by organic matter within the sulfidic zone of the sediment. Diffusive flux calculations as well as a mass balance that is based on the sedimentary Mo isotope composition suggest that about equal proportions of the Mo accumulating in the basin are delivered by Mn (oxyhydr)oxide minerals during inflow events and Mo scavenging with hydrogen sulfide during euxinic periods. Since the anoxic surface sediment where Mo is released from Mn (oxyhydr)oxides are separated by several centimeters from the deeper sulfidic layers where Mo is removed, the solid phase record of Mo concentration and isotope composition would be misinterpreted if steady state Mo accumulation was assumed. Based on our observations in the Gotland Deep, we argue that short-term redox fluctuations need to be considered when interpreting Mo-based paleo-records.

1. Introduction

1.1. Motivation

Over the last three decades significant progress has been made in the development of paleoceanographic proxies for the reconstruction of marine redox conditions in the past (e.g., Shaw et al., 1990; Calvert and Pedersen, 1993; Tribouillard et al., 2006; Brumsack, 2006). In particular the sedimentary concentration of trace metals such as Mo and uranium have proven useful as regional redox indicators because of their low background concentrations in terrigenous material as well as fundamentally reduced mobility upon transition from oxic to anoxic to

sulfidic conditions in the water column or sediments. Moreover, the isotope composition of these elements has been used as a (semi-) quantitative indicator for the global extent of seafloor area covered by anoxic bottom waters (e.g., Arnold et al., 2004; Wille et al., 2008; Montoya-Pino et al., 2010; Kendall et al., 2015; Dickson, 2017).

In applying these proxies, we typically assume that the signal reconstructed from trace metal concentrations or isotope ratios has been generated by a single mechanism (e.g., Mo scavenging under sulfidic conditions in the water column) that is linked to the long-term average redox-conditions (i.e., euxinia) rather than multiple mechanisms operating under different redox conditions (i.e., oxic and anoxic) and on different time scales (i.e., ranging from weeks to millennia). The time

* Corresponding author.

E-mail address: fscholz@geomar.de (F. Scholz).

<https://doi.org/10.1016/j.chemgeo.2018.04.031>

Received 22 February 2018; Received in revised form 24 April 2018; Accepted 26 April 2018

Available online 30 April 2018

0009-2541/ © 2018 Elsevier B.V. All rights reserved.

scales that proxy signals are extrapolated to inherently increase with the decreasing temporal resolution of sedimentary archives as we go back in geologic time. Any geochemical impact of shorter-term redox changes is therefore lumped together in a bulk signal which is interpreted as the result of a long-term steady state. In contrast to this common practice, many biogeochemical studies in modern sedimentary environments suggest that dynamic redox fluctuations, e.g., due to changes export production or circulation and ventilation, are common in many open-marine to weakly restricted marine systems (e.g., Huckriede and Meischner, 1996; Berelson et al., 2003; Scholz et al., 2011; Dale et al., 2017). Moreover, an increasing number of paleoceanographic studies report evidence for complex and temporally variable redox structures in past ocean basins (Poulton et al., 2010; Hammarlund et al., 2012; Westermann et al., 2014; Goldberg et al., 2016). The presence of multiple redox interfaces within a relatively short distance from each other makes it highly plausible that redox fluctuations, e.g., as a result of changes in export production or circulation pattern took place in these systems. However, because time series data for modern pore water and sediment geochemical parameters are scarce, the impact of redox fluctuations on the resulting isotope signature in sedimentary paleo-archives is difficult to ascertain.

Here we report the geochemistry of Mo and Mo isotopes in the

context of a recent seawater inflow and oxygenation events in the intermittently anoxic and sulfidic Gotland Deep (Fig. 1A, B) in the Central Baltic Sea. Comparing pore water and solid phase pattern of Mo and Mo isotopes before and during inflow and oxygenation provides unprecedented insights into how Mo-based proxy signatures are affected by short-term redox changes in the overlying water column.

1.2. Geochemistry of molybdenum and molybdenum isotopes

Molybdenum has a long residence time ($\sim 440,000$ years) (Miller et al., 2011) in oxygenated seawater and is uniformly distributed (~ 110 nM at a salinity of 35) in the global ocean (Bruland, 1983). In the presence of dissolved hydrogen sulfide ($\Sigma \text{H}_2\text{S} = \text{H}_2\text{S} + \text{HS}^- + \text{S}^{2-}$), molybdate (MoO_4^{2-}), the stable Mo species in oxygenated seawater, is converted to sulfur-containing Mo complexes (e.g., thiomolybdate ($\text{Mo}^{\text{VI}}\text{O}_x\text{S}_{4-x}^{2-}$, $1 < x < 4$) or Mo polysulfide ($\text{Mo}^{\text{IV}}\text{O}(\text{S}_4)\text{S}^{2-}$) (Helz et al., 1996; Erickson and Helz, 2000; Vorlíček et al., 2004; Dahl et al., 2013). Thiomolybdates or Mo polysulfides are particle reactive and show a strong affinity to iron (Fe) sulfide minerals and sulfur-rich organic matter (Huerta-Diaz and Morse, 1992; Zheng et al., 2000; Vorlíček and Helz, 2002; Vorlíček et al., 2004; Tribouillard et al., 2004; Helz et al., 2011; Wagner et al., 2017). Therefore, Mo is readily

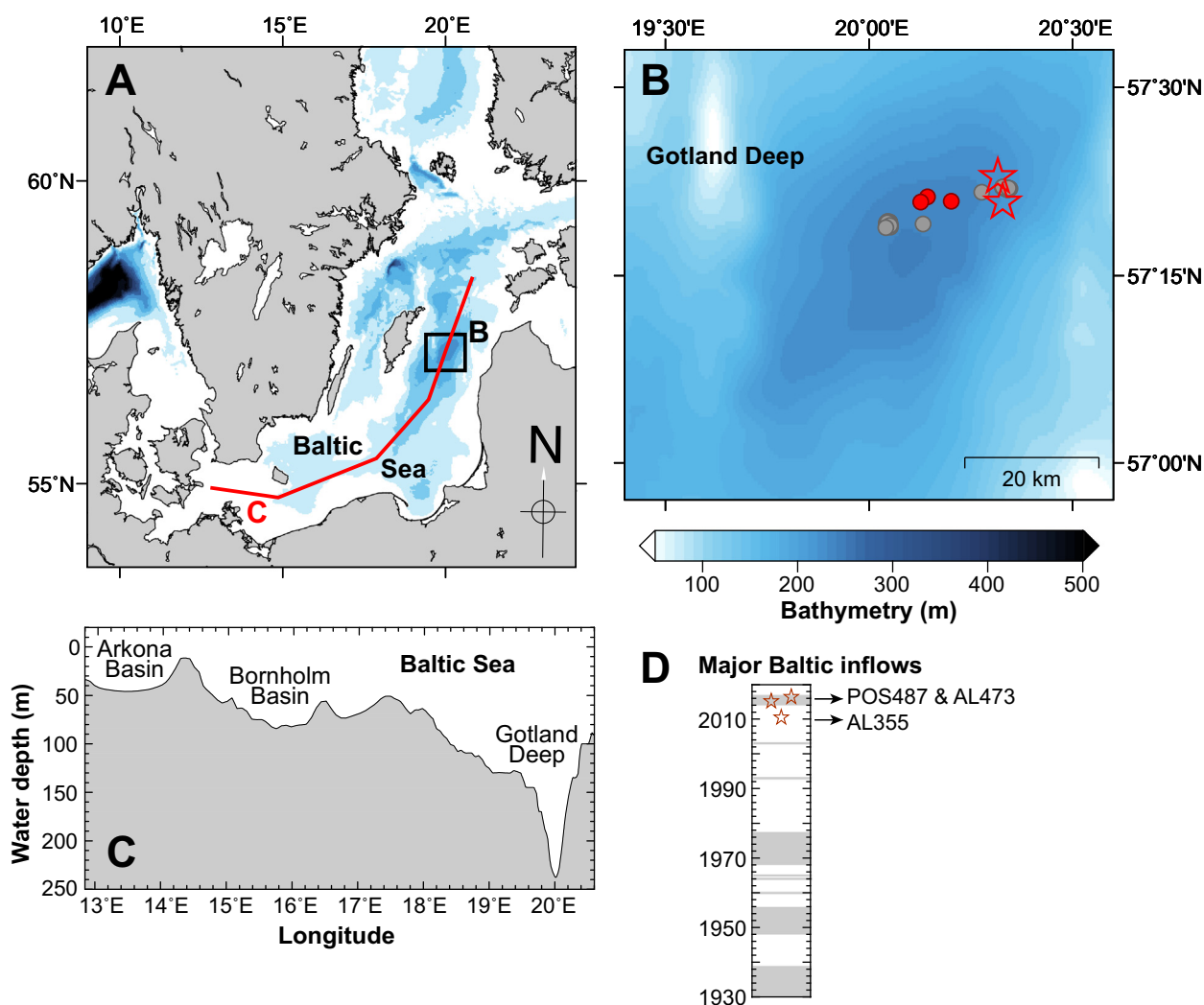


Fig. 1. (A) Bathymetric map of the Baltic Sea (bathymetric data from Seifert et al., 2001). (B) Close-up map showing the sampling locations within the Gotland Deep (red stars: sediment cores; red dots: CTD stations during cruises AL355, POS487 and AL473; gray dots: CTD stations during IOW cruises). (C) Bathymetric cross section through the Baltic Sea (see red line in (A)). (D) Record of major Baltic inflows since 1930 (based on data from Matthäus and Franck (1992), Matthäus et al. (2008) and the present study). Red stars in (D) depict the timing of sediment core retrieval during AL355, POS487 and AL473.

scavenged from sulfidic water columns and pore waters which results in sedimentary Mo enrichments. In some cases, sedimentary Mo enrichments in sulfidic environments can be masked by dilution with detrital material (Scott and Lyons, 2012). Moreover, sustained periods of Mo sequestration in anoxic and sulfidic basins with a long seawater residence time can lead to a depletion of the Mo inventory in the water column thus causing an attenuation of the Mo enrichment in the sediment (Algeo, 2004; Algeo and Lyons, 2006).

The relatively heavy Mo isotope composition of modern seawater ($\delta^{98}\text{Mo} = +2.3\text{‰}$) has been attributed to the balance between the terrigenous input flux supplied via weathering and river runoff (average $\delta^{98}\text{Mo}$ of $+0.7\text{‰}$) (Archer and Vance, 2008) and an isotopically light sink associated with Mo adsorption onto Mn (oxyhydr)oxides in well-oxygenated sediments in the deep-sea (Barling et al., 2001; Siebert et al., 2003). Another important Mo sink in the ocean are sulfidic continental margin sediments with oxic bottom water which are characterized by Mo isotope compositions intermediate between seawater and Mn (oxyhydr)oxides (mean $\delta^{98}\text{Mo}$ of approx. $+1.5\text{‰}$) (McManus et al., 2006; Poulson Brucker et al., 2009).

Early in the history of Mo isotope geochemical research, it was discovered that sediments in the euxinic Black Sea have a Mo isotope composition similar to oxic seawater implying near-quantitative conversion of dissolved MoO_4^{2-} to MoS_4^{2-} and removal with no expressed isotope fractionation when hydrogen sulfide is present in the water column (Barling et al., 2001; Arnold et al., 2004). Therefore, based on the assumption that sediments underneath euxinic waters generally record the Mo isotope composition of contemporary seawater, it was argued that if large parts of the ocean remained euxinic for a prolonged period of time the isotope composition of seawater would reach a new steady state value that lies closer to the $\delta^{98}\text{Mo}$ of the Mo input flux from rivers. Following this concept, black shales with a $\delta^{98}\text{Mo}$ below contemporary seawater combined with independent evidence for euxinic conditions (e.g., from Fe speciation) have been interpreted as a semi-quantitative indicator for more widespread euxinia during the corresponding intervals in Earth history (e.g., Arnold et al., 2004; Wille et al., 2008; Kendall et al., 2015; Goldberg et al., 2016). Importantly, however, the Black Sea is the only large euxinic basin investigated to date where the sedimentary Mo isotope signature below 400 m water depth reflects the $\delta^{98}\text{Mo}$ of contemporary seawater (Neubert et al., 2008). In most other euxinic basins investigated so far (e.g., Cariaco Basin, Baltic Sea Deep) $\delta^{98}\text{Mo}$ values span the entire range between the isotopically light oxic sink and modern seawater (Arnold et al., 2004; Neubert et al., 2008; Noordmann et al., 2015) thus implying partial removal of a fractionated Mo pool. In fact, the sedimentary Mo isotope values reported for most euxinic settings range between the Mo isotope values reported for oxic sediments (i.e., Mo associated with Mn (oxyhydr)oxides: $\delta^{98}\text{Mo} \approx -0.5\text{‰}$) and continental margin sediments where hydrogen sulfide is only present in the pore water ($\delta^{98}\text{Mo} \approx +1.5\text{‰}$).

Essentially two different mechanisms have been invoked to explain the Mo isotopic offset between sediments and seawater in euxinic basins or sulfidic sedimentary environments: The first explanation is related to an incomplete conversion of molybdate to thiomolybdate species followed by partial removal of the latter (Neubert et al., 2008; Dahl et al., 2010; Nagler et al., 2011). The change in aqueous Mo speciation is expected to be accompanied by isotope fractionation (Tossell, 2005) and should thus impart an isotopic offset in the solid phase if one of the species (i.e., MoS_4^{2-}) is preferentially removed. The conversion of MoO_4^{2-} to MoS_4^{2-} is a function of the hydrogen sulfide concentration. Thermodynamic constraints suggest that the conversion can proceed if aqueous H_2S concentrations ($\neq \Sigma\text{H}_2\text{S}$) exceed a threshold value of $11\text{ }\mu\text{M}$ (Helz et al., 1996). At ambient H_2S concentrations below this threshold, partial Mo removal may be accompanied by isotope fractionation thus leading to a lower sedimentary $\delta^{98}\text{Mo}$ than observed in the deep Black Sea. The second explanation is related to the deposition of a particulate phase where Mo is adsorbed to the surfaces

of metal (oxyhydr)oxides (McManus et al., 2002; Poulson Brucker et al., 2009; Goldberg et al., 2012; Scholz et al., 2017). Field data and experimental studies have demonstrated that light Mo isotopes preferentially adsorb to the surfaces of Mn and Fe (oxyhydr)oxide minerals. The extent of isotope fractionation decreases from Mn ($\Delta^{98}\text{Mo}_{\text{seawater-adsorbed}} = +2.8\text{‰}$) (Siebert et al., 2003; Barling and Anbar, 2004; Wasylenki et al., 2008) to Fe minerals ($\Delta^{98}\text{Mo}_{\text{seawater-adsorbed}} = +0.8$ to $+2.2\text{‰}$) and with decreasing crystallinity of the Fe (oxyhydr)oxides: hematite ($\Delta^{98}\text{Mo}_{\text{seawater-adsorbed}} = +2.19 \pm 0.54\text{‰}$) > goethite ($\Delta^{98}\text{Mo}_{\text{seawater-adsorbed}} = +1.40 \pm 0.48\text{‰}$) > ferrihydrite ($\Delta^{98}\text{Mo}_{\text{seawater-adsorbed}} = +1.11 \pm 0.15\text{‰}$) (Goldberg et al., 2009). Release of Mo from Mn and/or Fe (oxyhydr)oxides followed by interaction with pore water sulfide and precipitation of an authigenic Mo phase would thus also produce a lighter Mo isotope value than seawater.

Both mechanisms outlined above are particularly relevant in intermittently euxinic basins such as the Gotland Deep. Occasional exchange of the anoxic deep water may limit the accumulation of hydrogen sulfide thus impeding quantitative conversion of MoO_4^{2-} to MoS_4^{2-} (Neubert et al., 2008; Nagler et al., 2011). Moreover, due to lateral supply of Mn (oxyhydr)oxide minerals and reductive dissolution within the anoxic water column, intermittently euxinic basins are typically characterized by elevated concentrations of dissolved Mn compared to unrestricted, well-oxygenated environments (Calvert and Pedersen, 1996). This is particularly the case in the Baltic Sea where the shallow Mn source area is relatively large compared to the anoxic Deep (Jilbert and Slomp, 2013a; Scholz et al., 2013). The dissolved Mn pool within the euxinic deep water is occasionally re-oxidized and precipitated, either due to inflow of oxygenated seawater or vertical transport across the anoxic-oxic interface (Calvert and Pedersen, 1996; Huckriede and Meischner, 1996; Neumann et al., 2002; Dellwig et al., 2010). The Mn (oxyhydr)oxide minerals formed by these mechanisms scavenge Mo which is then shuttled into the deep water or to the sediment surface (Berrang and Grill, 1974; Jacobs et al., 1987; Algeo and Tribouillard, 2009; Dellwig et al., 2010). Both Mo removal from weakly sulfidic waters and Mo scavenging by metal (oxyhydr)oxides has been invoked to explain the Mo isotope composition of sediments in the Gotland Deep in previous studies (Neubert et al., 2008; Nagler et al., 2011; Scholz et al., 2013; Noordmann et al., 2015). Our data will allow us to better constrain the detailed mechanism by which Mo isotope signatures are recorded in Gotland Deep sediments.

2. Study area

The Baltic Sea (Fig. 1A) is one of the world ocean's largest brackish water basins. The estuarine circulation pattern and semi-enclosed character of the Baltic Sea promote vertical stratification and oxygen depletion below the pycnocline (Zillen et al., 2008). Because of the characteristic bathymetry of the Baltic Sea (Fig. 1C), euxinic conditions occur in sub-basins (so-called “Deep”) among which the Gotland Deep is the largest by area (Fig. 1B). The Gotland Deep has an aerial extent of $\sim 4600\text{ km}^2$ below the 150 m isobath and a maximum water depth of $\sim 250\text{ m}$ (Siebert et al., 2001). The intensity and aerial extent of anoxia in the Baltic Sea has progressively increased since the industrial revolution (Zillen et al., 2008; Conley et al., 2009). This trend is generally attributed to eutrophication resulting from external nutrient inputs as well as the amplifying effect of enhanced phosphorous recycling from anoxic sediments (Conley et al., 2002, 2009; Jilbert et al., 2011; Jilbert and Slomp, 2013a; Noffke et al., 2016; Sommer et al., 2017).

The water column redox structure of the Gotland Deep is affected by occasional inflow events of saline and well-oxygenated water from the North Sea. During such “major Baltic inflows” (MBI) (Matthaus and Franck, 1992; Matthaus et al., 2008), North Sea water penetrates the Baltic Sea through the Danish Straits and, depending on the pre-existing density stratification, progressively propagates into the more distal Baltic Deep (Fig. 1C) (Matthaus et al., 2008). After the Gotland Deep

Table 1
Station list.

Cruise	Station	Device	Sampling date	Longitude N	Latitude E	Water depth (m)
MUCs						
AL355	345	MUC05	6/8/2010	57°22.99'	20°18.98'	223
POS487	444	MUC20	8/5/2015	57°22.99'	20°18.97'	228
AL473	130	MUC12	3/21/2016	57°20.89'	20°19.98'	219
CTDs						
AL355	335	CTD07	6/5/2010	57°21.31'	20°08.62'	235
POS487	353	CTD19	7/22/2015	57°20.89'	20°07.60'	242
AL473	133	CTD20	3/21/2016	57°20.93'	20°12.11'	236

has been flushed with saline and well-oxygenated water, the deep water remains oxic for a period of several months before anoxia and eventually euxinia re-establishes (Matthäus et al., 2008). The occurrence, intensity and velocity of inflow events chiefly depend on the balance between the favoring effect of westerly winds and the impeding effect of freshwater runoff from the Baltic Sea drainage area (Schinke and Matthäus, 1998). Through the late 1970s, MBIs occurred frequently, either as single events (e.g., 1960, 1965; Fig. 1D) or groups of events (e.g., 1931–1938, 1948–1956, 1968–1978; Fig. 1D) (Matthäus and Franck, 1992; Matthäus et al., 2008). Since then, only a few isolated events (mainly 1993 and 2003) have been observed. After about 10 years without a major Baltic inflow, several consecutive events took place between 2014 and 2017 (Gräwe et al., 2015; Mohrholz et al., 2015; Naumann et al., 2017). In the present study, we will compare pore water and solid phase data of sediment cores which were taken before and during this series of inflow events (see Table 1 for details).

3. Methods

The sediments cores used in this study were retrieved with a multiple corer (MUC) during research cruises in June 2010 (RV Alkor cruise AL355), July/August 2015 (RV Poseidon cruise POS487) and March 2016 (AL473). Each MUC deployment was accompanied by a CTD rosette deployment for the measurement of salinity and oxygen concentrations in the water column. Sediment and water column geochemical data for samples obtained during AL355 were previously published in Scholz et al. (2013). The distribution of oxygen in the water column during POS487 and AL473 was described by Sommer et al. (2017). Additional salinity and oxygen data in the Gotland Deep for the time period between February 2010 and August 2016 were collected in the framework of the long-term data program conducted by the Leibniz-Institute for Baltic Sea Research Warnemünde (IOW).

During cruises AL355 pore waters were extracted using rhizon samplers. On the other cruises, sediment cores were sliced in an argon-flushed glove bag and the pore water was extracted in a second glove bag by using a sediment squeezer. Pore waters for metal analyses were acidified with concentrated HNO₃ (sub-boiled distilled) and stored in acid-cleaned polypropylene vials until further treatment after the cruise. Pore water sulfate (SO₄^{2−}) and chloride concentrations were analyzed by ion chromatography. Salinity was calculated from chlorinity by applying the conservative chloride to salinity relationship in seawater. Hydrogen sulfide (ΣH₂S) concentrations in the water column and pore waters were determined photometrically by applying the methylene blue method (Grasshoff et al., 2002). Concentrations of Fe and Mn were analyzed by inductively coupled plasma optical emission spectroscopy (ICP-OES, VARIAN 720-ES) or, at concentrations below 5 μM (Fe) and 1 μM (Mn), by inductively coupled plasma mass spectrometry (ICP-MS, Agilent Technologies 7500 Series). Measurements of dissolved Fe by ICP-MS were performed in H₂ collision mode to avoid possible argon oxide interferences. All samples and standards were spiked with an yttrium standard in order to internally normalize for

varying ionization efficiency. The standards were prepared with an appropriate amount of artificial seawater to match the sample salinity. Dissolved Mo concentrations were analyzed by isotope dilution ICP-MS. The seawater standards CASS-5 (measured value: 103.0 ± 0.9 nM, n = 6; recommended value 103 nM) and NASS-6 (103.7 ± 1.7 nM, n = 6; certified value 100.7 ± 7.3 nM) from the Canadian Research Council were measured repeatedly to assess the accuracy and precision of this method.

Sediment samples were stored in pre-weighed plastic cups for the determination of water content and porosity. Concentrations of total carbon and total sulfur (TS) were determined with an element analyzer (Euro EA, HEKATEch). Inorganic carbon was driven out with HCl prior to TOC analysis and total inorganic carbon (TIC) was obtained by subtracting TOC from total carbon. For the analysis of total element concentrations, freeze-dried and ground sediment samples were treated with hydrofluoric acid (40%, trace metal grade), nitric acid (65%, sub-boiled distilled) and perchloric acid (60%, pro analysis) on a hotplate and the resulting solutions were analyzed by ICP-OES (Al, Mn and Fe) and ICP-MS (Mo). For quality control, reference standards MESS-3 (marine sediment, Canadian Research Council) and SCO-1 (Cody Shale, USGS) were digested and analyzed along with sediment samples. Certified and measured concentrations are summarized in Table 2.

To discriminate authigenic element enrichments against the lithogenic background, Mn and Fe concentrations are normalized to Al and the resulting ratios are compared to those of the upper continental crust (Mn/Al = 7.46 · 10^{−3}, Fe/Al = 0.44) (McLennan, 2001). Sedimentary Mo concentrations are reported as excess concentration (Eq. 1) above the upper continental crust (Mo/Al = 1.87 · 10^{−5}) (McLennan, 2001):

$$Mo_{XS} = Mo_{sample} - \frac{Mo_{crust}}{Al_{crust}} \cdot Al_{sample} \quad (1)$$

Mo isotope compositions were analyzed on a Nu Instruments MC-ICPMS with DSN-100 Desolvation Nebulizer System (GEOMAR, Kiel) employing a Mo isotope double spike (¹⁰⁰Mo, ⁹⁷Mo) for correction of instrumental mass bias and possible mass fractionation during chemical separation of Mo from the matrix (Siebert et al., 2001). Chemical separation was performed in 0.5 M HCl on 2 mL of Biorad AG50W-X8 cation resin to remove Fe, followed by separation from the remaining matrix in 4 M HCl on 1 mL Biorad AG1-X8 anion exchange resin and elution in 2 M HNO₃. Total procedural blanks were < 1 ng of Mo. During measurements of sediment samples a total of 50 ng of Mo was analyzed resulting in ion beam intensities of 100 to 140 V ppm^{−1} (excluding double spike signal) using 10¹¹ Ω resistors. Each measurement is the average of 4 blocks of 10 measurement cycles with 10 s signal integration time each. Mass 99 was monitored for possible isobaric interferences of ruthenium.

All Mo isotopic variations are presented in delta notation as the deviation of the ⁹⁸Mo/⁹⁵Mo ratio in parts per thousand (‰) relative to a standard:

Table 2
Certified and measured element concentrations in reference standards.

	Al (wt%)	Fe (wt%)	Mn (mg g ^{−1})	Mo (μg g ^{−1})
MESS-3				
Certified value	8.59 ± 0.23	4.34 ± 0.11	0.324 ± 0.012	2.78 ± 0.07
Measured value (n = 3)	8.50 ± 0.12	4.24 ± 0.15	0.317 ± 0.003	2.79 ± 0.05
SCO-1				
Certified value	7.50 ± 0.11	3.59 ± 0.13	0.410 ± 0.030	1.40 ± 0.20
Measured value (n = 3)	7.25 ± 0.09	3.58 ± 0.46	0.394 ± 0.003	1.26 ± 0.02

$$\delta^{98}\text{Mo} = \left(\frac{\left(\frac{{}^{98}\text{Mo}}{{}^{95}\text{Mo}} \right)_{\text{sample}}}{\left(\frac{{}^{98}\text{Mo}}{{}^{95}\text{Mo}} \right)_{\text{standard}}} - 1 \right) \cdot 1000 \quad (2)$$

Samples were measured relative to Alfa Aesar Mo plasma standard solution Specpure #38791 (lot no. 011895D) (see discussion in Nagler et al. (2014)). International standard NIST-SRM-3134 was measured constantly and has an offset from the Alfa Aesar standard of $+0.15 \pm 0.08\text{‰}$ (2SD, $n = 46$), which is in agreement with published values of Greber et al. (2012) and Nagler et al. (2014). Following Nagler et al. (2014), we present the results in the delta notation relative to the NIST-SRM-3134 scale with an offset of $+0.25\text{‰}$. This allows us to discuss changes in Mo isotope values relative to long established values of, for example, a $\delta^{98}\text{Mo}$ of $+2.3\text{‰}$ for seawater and makes results comparable to earlier studies on oceanic Mo isotope fractionation. USGS rock standard reference material SDO-1 (black shale) was processed through chemistry and measured with each sample run. The long-term external reproducibility of SDO-1 is 0.09‰ (2 SD, average $\delta^{98}\text{Mo}$ is $+0.99\text{‰}$). The long-term external reproducibility of the Specpure standard solution is $< 0.1\text{‰}$ (2 SD).

A number of pore water samples with sufficiently high volume and Mo concentration were selected for pore water Mo isotope analyses. Unfortunately, the pore water Mo concentrations of samples from cruise AL355 (and the amount of pore water leftover, respectively) were too low for Mo isotope analyses. Pore water Mo isotope analyses were performed as described above for sediment samples. The analytical blank was $< 1 \text{ ng}$.

4. Results and discussion

4.1. Evolution of water column redox conditions

During cruise AL355 in June 2010, the water column of the Gotland Deep was characterized by anoxic conditions below the halocline ($> 100 \text{ m}$ water depth) (Fig. 2A, B). The boundary between non-sulfidic and sulfidic water (chemocline) was located at 120 m water depth and the $\Sigma\text{H}_2\text{S}$ concentration increased to maximum values of $\sim 120 \mu\text{M}$ in the deepest part of the basin (Fig. 2C). This water column redox structure is typical for stagnant periods in the Gotland Deep (Neretin

et al., 2003; Dellwig et al., 2010; Ulfssbo et al., 2011; Meyer et al., 2012) and consistent with the long-term salinity and oxygen record compiled by the IOW (Fig. 3), which is based on multiple CTD casts in the vicinity of our sediment core locations (Fig. 1). As indicated by rising salinity values and oxygen concentrations (Fig. 3), seawater inflow started early in 2014 and continued as a series of MBIs and smaller events up to spring 2017 (Grawe et al., 2015; Mohrholz et al., 2015; Naumann et al., 2017). At the time of the cruises POS487 in July/August 2015 and AL473 in March 2016, the deep water ($> 200 \text{ m}$ water depth) of the Gotland Deep was characterized by variable oxygen concentrations ranging from $\sim 20 \mu\text{M}$ to $\sim 60 \mu\text{M}$ (Fig. 2B). The long-term oxygen record suggests that the deep water was transiently anoxic in between these two cruises (Fig. 3C).

4.2. Solid phase geochemical records

All sediment cores investigated in this study display a characteristic transition from low TOC and close to zero Mo_{XS} concentrations at the lower end of the core to high TOC ($\sim 10\text{--}15 \text{ wt}\%$) and Mo_{XS} ($100\text{--}200 \mu\text{g g}^{-1}$) within the uppermost 10 cm (Fig. 4). The increase in sediment TOC reflects the progressive intensification of hypoxia and associated increase in organic carbon delivery and preservation over the 20th century (Leipe et al., 2008). Bacterial sulfate reduction drives organic matter degradation in the sediment. Therefore, the increase in organic carbon delivery resulted in increasing hydrogen sulfide concentrations within the pore water and, consequently, in increased rates of authigenic Mo sequestration in the sediment (Jilbert and Slomp, 2013b; Scholz et al., 2013). Based on the well-known connection between recent environmental change and the accumulation of organic carbon and redox-sensitive trace metals such as Mo in sediments of the Gotland Deep, we infer that our sedimentary records cover a time period of approximately 100 years. This age constraint is consistent with sedimentation rates derived from radiometric dating published in earlier studies (Leipe et al., 2008; Hille et al., 2006).

Both Mn and Fe are strongly enriched over the lithogenic background in sediments of the Gotland Deep (Fig. 4). Previous studies have demonstrated that the excess Mn and Fe is transferred from shallower areas above the chemocline through lateral transport in the water column and trapping within the anoxic deep water and sediments (e.g.,

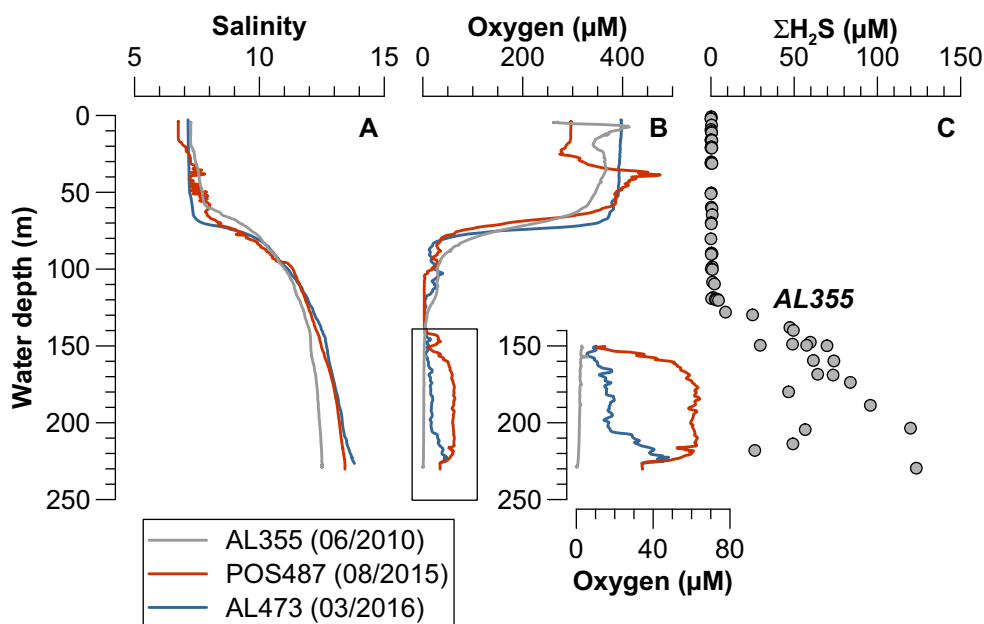


Fig. 2. Profiles of (A) salinity, (B) oxygen and (C) $\Sigma\text{H}_2\text{S}$ in the water column of the Gotland Deep during cruises AL355, POS487 and AL473. The close-up in (B) shows the oxygen distribution within the deepest part of the basin in detail. Note that water column hydrogen sulfide was only detected during AL355.

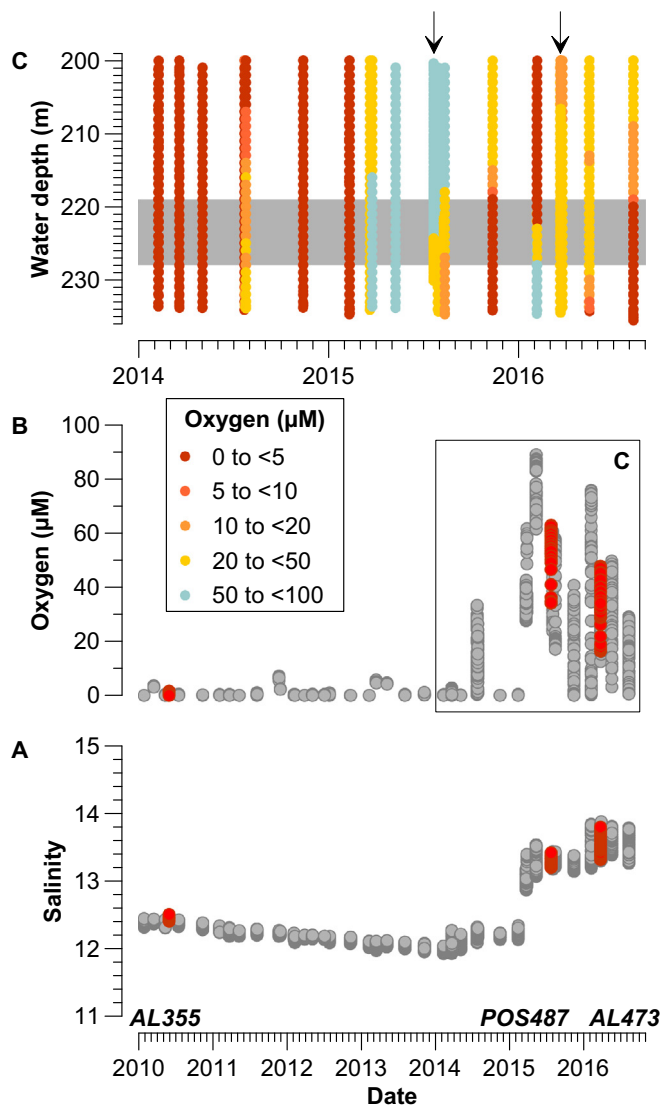


Fig. 3. Evolution of (A) salinity and (B) oxygen concentration below 200 m water depth in the Gotland Deep between 2010 and 2017 (red dots: CTD data from cruises AL355, POS487 and AL473; gray dots: CTD data from IOW cruises). (C) Close-up of the oxygen distribution below 200 m water depth during the inflow period (2014–2016). The gray array depicts the water depth of the sediment cores investigated in this study. Vertical arrows depict the timing of the research cruises POS487 and AL473.

Fehr et al., 2008, 2010; Jilbert and Slomp, 2013a; Scholz et al., 2013; Lenz et al., 2015a). This mechanism is generally referred to as a “shelf-to-basin shuttle” (Raiswell and Anderson, 2005; Lyons and Severmann, 2006). The distributions of Mn/Al and Fe/Al are closely related to the distribution of inorganic carbon and total sulfur, respectively (Fig. 4). These co-variation patterns corroborate the findings of earlier studies which demonstrated that Mn is mainly present as carbonate (calcium-rich rhodochrosite) whereas Fe is bound to sulfide minerals (pyrite) (Suess, 1979; Boesen and Postma, 1988; Huckriede and Meischner, 1996; Sternbeck and Sohlenius, 1997; Neumann et al., 2002).

The formation of Mn carbonate in sediments of the Baltic Deep is closely related to inflow and oxygenation events. During anoxic periods, laterally supplied Mn (oxyhydr)oxides are trapped and dissolved within the anoxic basin. Upon seawater inflow and oxygenation, the dissolved Mn that has accumulated within the deep water is oxidized and deposited at the basin floor. As anoxia re-establishes Mn (oxyhydr)oxides are again dissolved and the Mn released into the pore water is

partly recycled into the bottom water whereas the remainder is precipitated with bicarbonate as Ca-rich rhodochrosite (Jakobsen and Postma, 1989; Sternbeck and Sohlenius, 1997; Neumann et al., 2002). The distinct layers of Mn carbonate observed in sediments of the Gotland Deep have been proposed as paleo-indicators for seawater inflow (Neumann et al., 1997). Consistent with the age constraints from TOC and Mo_{XS} , the pronounced Mn and TIC peaks observed at 15 to 20 cm depth in all three cores are assigned to the period with frequent inflow and oxygenation vents in the 1950s through 1970s (Fig. 1D) (Neumann et al., 1997). In the shallower portion of the cores, Mn and TIC peaks are less pronounced and less well correlated. We infer that is related to the reduced frequency of inflow events and shorter duration of oxic periods since the end of the 1970s (Fig. 1D). According to Heiser et al. (2001) single inflow events cannot generate a durable Mn carbonate peak as most of the fresh rhodochrosite is re-suspended and dissolved shortly after formation. Moreover, increased formation of hydrogen sulfide within the sediment as a result of intensifying hypoxia and increased organic matter availability over the last decades may have led to accelerated chemolithoautotrophic Mn reduction in the surface sediment and thus reduced sedimentary Mn sequestration (Lenz et al., 2015b).

Coincident maxima of Mn/Al and Fe/Al suggest that, in analogy to Mn, the rate of Fe deposition is also increased during oxygenation events. This assumption is supported by elevated concentrations of dissolved Fe (1–2 μM) (Dyrssen and Kremling, 1990; Meyer et al., 2012; Pohl and Fernández-Otero, 2012) in the water column during anoxic periods which may be precipitated as Fe (oxyhydr)oxide and deposited upon inflow of oxygenated seawater. In contrast to Mn, however, Fe is also precipitated from the anoxic water column via syngenetic pyrite formation (Boesen and Postma, 1988; Fehr et al., 2008, 2010). Therefore, Fe/Al maxima are generally less pronounced and not always aligned with Mn/Al maxima (Fig. 4).

We observe a close correlation between sedimentary Mo and TOC concentrations ($R^2 = 0.74$) in the Gotland Deep suggesting that organic material rather than Fe sulfide minerals (Mo versus Fe/Al or TS: $R^2 < 0.01$) represent the ultimate burial phase of Mo. This assumption is consistent with several studies which provided direct (from x-ray absorption spectroscopy) or indirect (Mo-TOC correlation) evidence for the association of Mo with sulfide-containing organic material in sediments of euxinic basins and lakes (Algeo and Lyons, 2006; Wagner et al., 2017; Dahl et al., 2017). However, the apparent association of Mo with organic material within the sediment does not necessarily imply a joint delivery of Mo and organic material to the sediment surface. In the following, we discuss evidence for different modes of Mo delivery and the magnitude of the associated Mo fluxes based on pore water chemistry.

4.3. Pore water geochemistry and early diagenesis

Prior to the inflow events (AL355), pore water Mo concentrations were mostly similar to or below the salinity-normalized value (Fig. 5). This observation could indicate that either little Mo was released into the pore water or that Mo was efficiently removed from the pore water. Both of these explanations are supported by the pore water Mn and $\Sigma\text{H}_2\text{S}$ data (Fig. 5). Hydrogen sulfide concentrations increase shortly below the sediment-water interface indicating that Mo could be efficiently removed. Moreover, the lack of a surficial pore water Mn peak indicates that there was little Mn (oxyhydr)oxide dissolution at the surface which could have released Mo into the pore water. Instead, the Mn profile is characterized by a steady increase below the sediment-water interface. The deep-sourced Mn flux implied by this profile is typical for anoxic periods in the Gotland Deep and has been attributed to re-crystallization of Ca-rich rhodochrosite below the recovered sediment depth interval (Jakobsen and Postma, 1989; Sternbeck and Sohlenius, 1997; Jilbert and Slomp, 2013a).

After seawater inflow (POS487, AL473), pore water Mo profiles

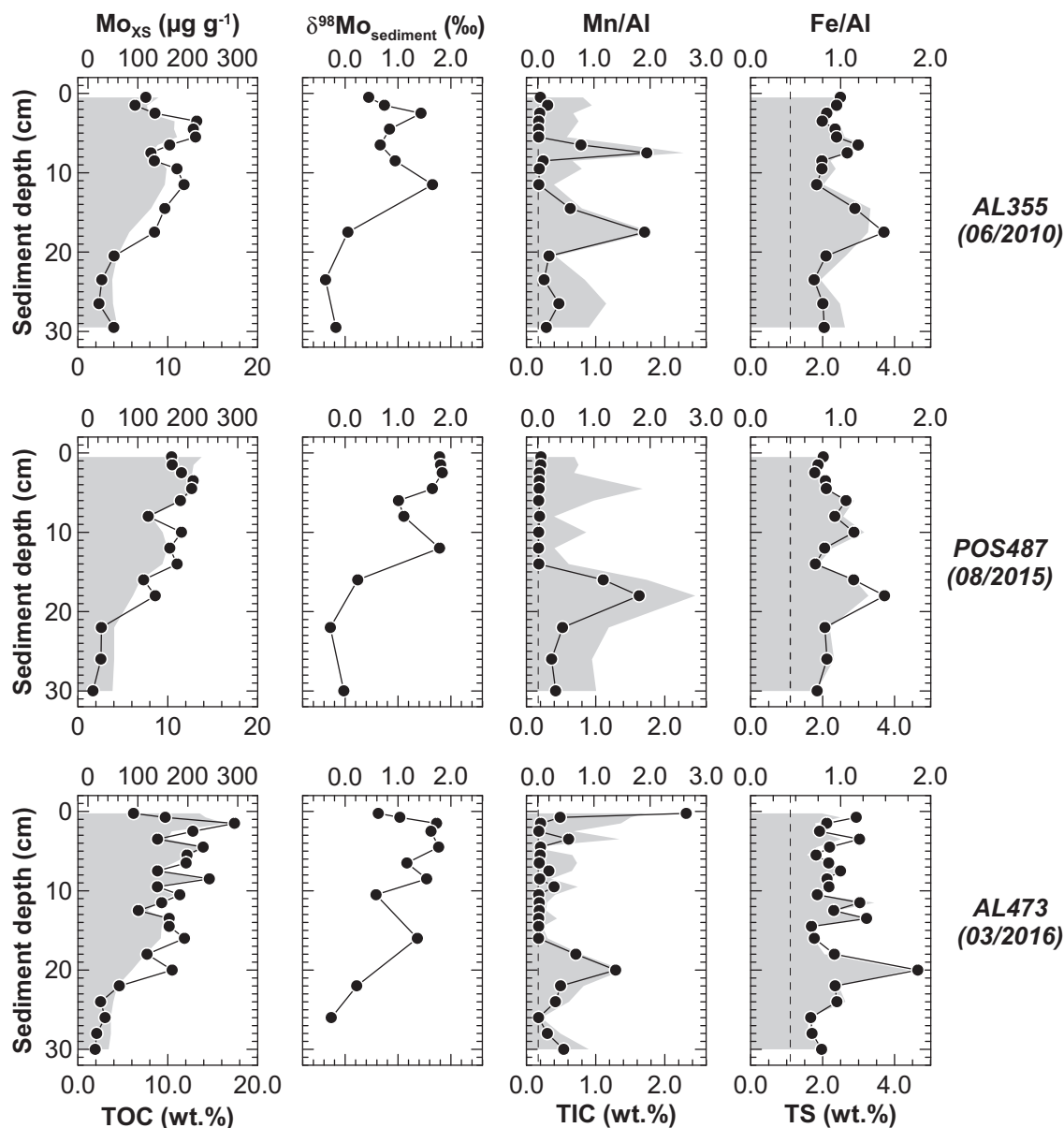


Fig. 4. Solid phase profiles of (left column) Mo_{XS} , TOC (shading), (central left column) $\delta^{98}\text{Mo}_{\text{sediment}}$, (central right column) Mn/Al, TIC, (right column) Fe/Al and TS (shading) for sediment cores taken before (AL355) and after (POS487, AL473) inflow. Vertical dashed lines represent the Mn/Al and Fe/Al of the upper continental crust (McLennan, 2001). Note that the uppermost 2 to 3 cm of fluid mud of the POS487 core were lost during core recovery. The data shown in this figure are contained in the Electronic Annex.

display pronounced peaks close the sediment surface (Fig. 5). Within these maxima, Mo concentrations exceed the salinity-normalized value by more than two orders of magnitude. The pore water Mo peaks coincide with maxima in pore water Mn suggesting that the excess Mo in pore water is released from Mn (oxyhydr)oxide minerals which precipitated and adsorbed Mo in the water column during inflow of oxygenated seawater. The pore water Mn peaks are relatively broad and the Mn profiles progressively re-adjust to the Mn gradient that was observed prior to the inflow events below 10 to 15 cm sediment depth (dashed lines in the Mn diagrams in Fig. 5). This observation is consistent with Heiser et al. (2001) who argued that Mn removal from pore water and fixation in the sediment as Mn carbonate is relatively inefficient so that much of the Mn delivered during inflow events is lost by diffusion across the sediment-water interface. By contrast, Mo concentrations drop sharply below the surficial maximum and reach values close to the salinity-normalized concentration at 5 to 10 cm sediment depth. This sharp decline in Mo concentration coincides with increasing

concentrations of $\Sigma\text{H}_2\text{S}$ (Fig. 5). This observation, combined with the close correlation between solid phase Mo and TOC throughout the sediment column (see Section 4.2), suggests that much of the Mo delivered by Mn (oxyhydr)oxides during inflow events interacts with pore water sulfide and is sequestered by organic material.

We can evaluate the contribution of Mo delivered by Mn (oxyhydr)oxides during inflow events to the overall Mo mass accumulation rate by calculating the diffusive Mo flux from pore water concentration gradients according to Fick's 1st Law:

$$F_{\text{Mo}} = -\phi \cdot D_{\text{sed}} \cdot \frac{d[\text{Mo}]}{dx} \quad (3)$$

In this equation, ϕ is porosity, D_{sed} is the diffusion coefficient for Mo in sediment and $d[\text{Mo}]/dx$ denotes the Mo concentration gradient from the Mo maximum to the intercept with the $\Sigma\text{H}_2\text{S}$ gradient (see down arrows in Fig. 6). The diffusion coefficient for Mo in seawater (D_{SW}) (Li and Gregory, 1974) was adjusted to in situ temperature and pressure

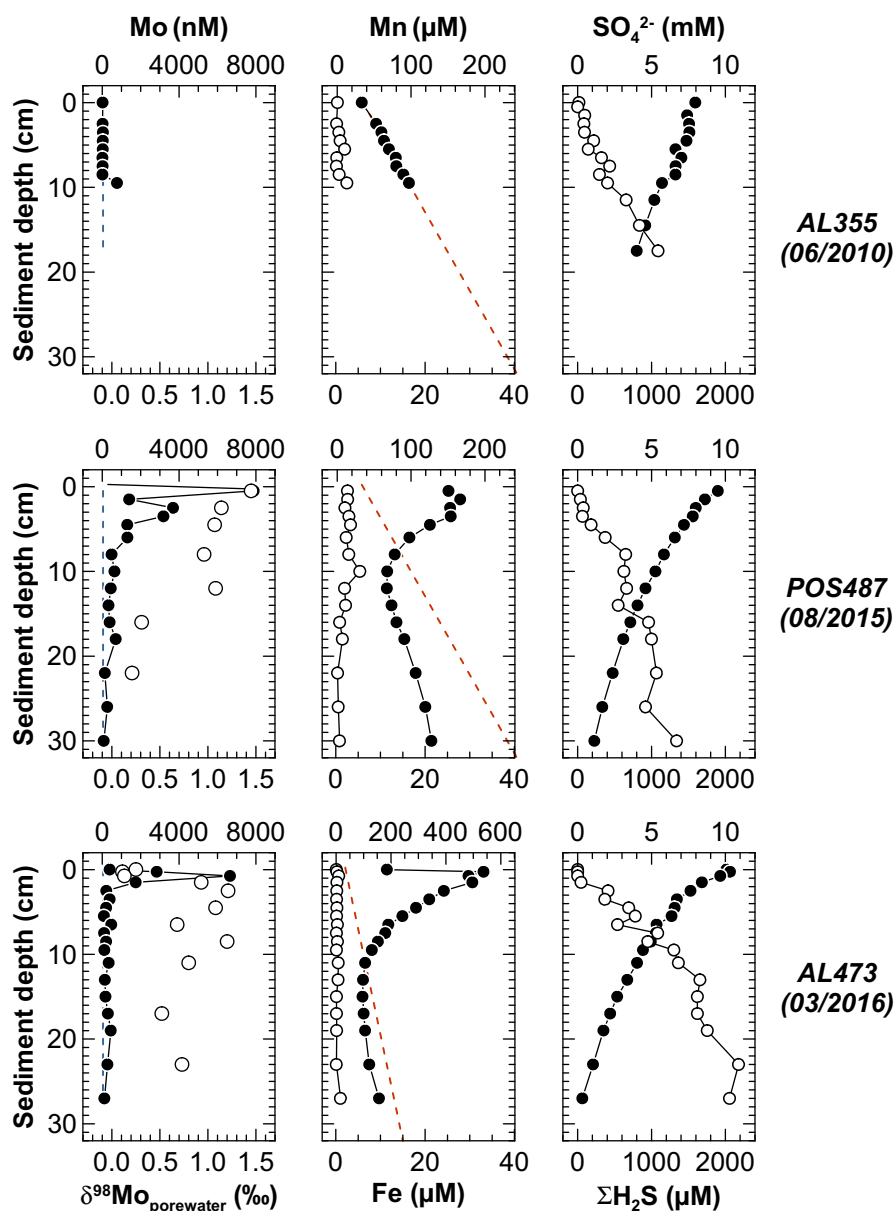


Fig. 5. Pore water profiles of (left column) Mo (closed symbols) and $\delta^{98}\text{Mo}_{\text{pore water}}$ (open symbols) (central column) Mn (closed symbols) and Fe (open symbols), (right column) SO_4^{2-} (closed symbols) and $\Sigma\text{H}_2\text{S}$ (open symbols) for sediment cores taken before (AL355) and after (POS487, AL473) inflow. The uppermost samples in each profile (depth of zero) represent the bottom water. Dashed lines in left column depict salinity-related Mo concentrations. Dashed lines in central column depict the Mn gradient prior to the inflow period. Note that the bottom water and uppermost 2 to 3 cm of fluid mud of the POS487 core were lost during core recovery. The data shown in this figure are contained in the Electronic Annex.

using the Stokes-Einstein equation and converted to D_{sed} as follows:

$$D_{\text{sed}} = \frac{D_{\text{sw}}}{\theta^2} \quad (4)$$

Tortuosity (θ^2) was derived from porosity using the following relationship from Boudreau (1996):

$$\theta^2 = 1 - \ln(\phi^2) \quad (5)$$

Importantly, the Mo peak observed in the aftermath of oxygenation events is a transient feature and will dissipate over time due to Mo removal with hydrogen sulfide and organic matter as well as upward diffusion across the sediment-water interface. The time over which excess Mo will disappear from the pore water will depend on the balance between the rate of Mo release from Mn (oxyhydr)oxides and the hydrogen sulfide flux from below which is ultimately driven by organic matter degradation. During our two sampling campaigns in August 2015 (POS487) and March 2017 (AL473), the Mo gradient and corresponding diffusive Mo flux from the surface sediment into the sulfidic zone of the sediment was remarkably similar (Table 3). As the bottom became again anoxic in between our two campaigns (Fig. 3C), multiple cycles of Mn dissolution in the sediment and re-precipitation in the

bottom water may have helped to maintain the diffusive Mo flux over a time period of several months. By contrast, other relatively recent inflow and oxygenation events in 2003 and 1993 were shorter in duration which is why the Mo peak in the pore water likely dissipated more rapidly.

Multiplying the average sediment mass accumulation rate in the Gotland Deep below 150 m water depth ($129 \pm 112 \text{ g m}^{-2} \text{ yr}^{-1}$) (Hille et al., 2006) by the average Mo concentration in the uppermost 15 cm of our sediment cores ($172 \pm 43 \mu\text{g g}^{-1}$) yields an approximate Mo mass accumulation rate at our study site of $2.31 \cdot 10^2 \mu\text{mol m}^{-2} \text{ yr}^{-1}$. Dividing the inflow-related diffusive Mo flux (Table 3) by the total annual Mo mass accumulation rate reveals that the Mo accumulating through inflow-related diffusion over one month (i.e., F_{Mo} in $\mu\text{mol m}^{-2} \text{ yr}^{-1}$ divided by 12, which is a conservative estimate of the longevity of the Mo peak) corresponds to the amount of solid phase Mo accumulating, on average, over a time period of 4 years. The average deep water residence time in the Gotland Deep is 20 years (Reissmann et al., 2009). This relatively short residence time is related to the occasional occurrence of inflow (and oxygenation) events. In fact, without regular inflow of seawater, the deep water residence time would be on

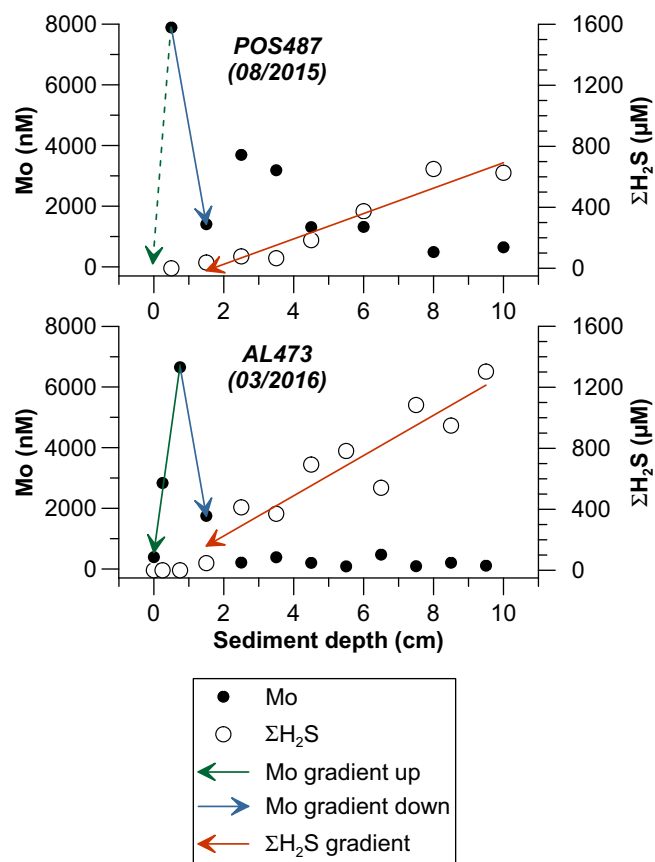


Fig. 6. Plot of dissolved Mo and $\Sigma\text{H}_2\text{S}$ versus sediment depth for the uppermost 10 cm of the cores taken after inflow (POS487, AL473) (see Fig. 5 for full pore water profiles). Arrows depict the concentration-depth gradients referred to in the discussion and used in diffusive flux calculations (Table 3). Note that the bottom water and uppermost 2 to 3 cm of fluid mud of the POS487 core were lost during core recovery.

the order of 100 years (Feistel et al., 2006). Taking the frequency and duration of inflow events into account, our flux calculations strongly suggest that Mo scavenging by Mn (oxyhydr)oxides contributes significantly to the total Mo burial flux in Gotland Deep sediments. In the following section we will evaluate how this mode of Mo delivery affects the sedimentary record of Mo isotopes.

4.4. Influence of seawater inflow on sedimentary molybdenum isotope cycling

All three sediment cores display similar downcore patterns of solid phase $\delta^{98}\text{Mo}$. Sediments with low TOC and Mo concentrations close to the base of the cores (> 20 cm sediment depth) are characterized by negative $\delta^{98}\text{Mo}_{\text{sediment}}$ values ($-0.15 \pm 0.22\text{‰}$, 1 SD, $n = 6$) (Fig. 4). This range of Mo isotope values resembles those observed in oxic deep-sea sediments of the Pacific Ocean ($\delta^{98}\text{Mo}_{\text{sediment}} = \sim -0.5\text{‰}$) where seawater Mo is adsorbed to Mn (oxyhydr)oxides at the sediment surface. As these mineral coatings are in contact with an infinite reservoir of seawater Mo ($\delta^{98}\text{Mo}_{\text{seawater}} = +2.3\text{‰}$), the full $\Delta^{98}\text{Mo}_{\text{seawater-adsorbed}}$

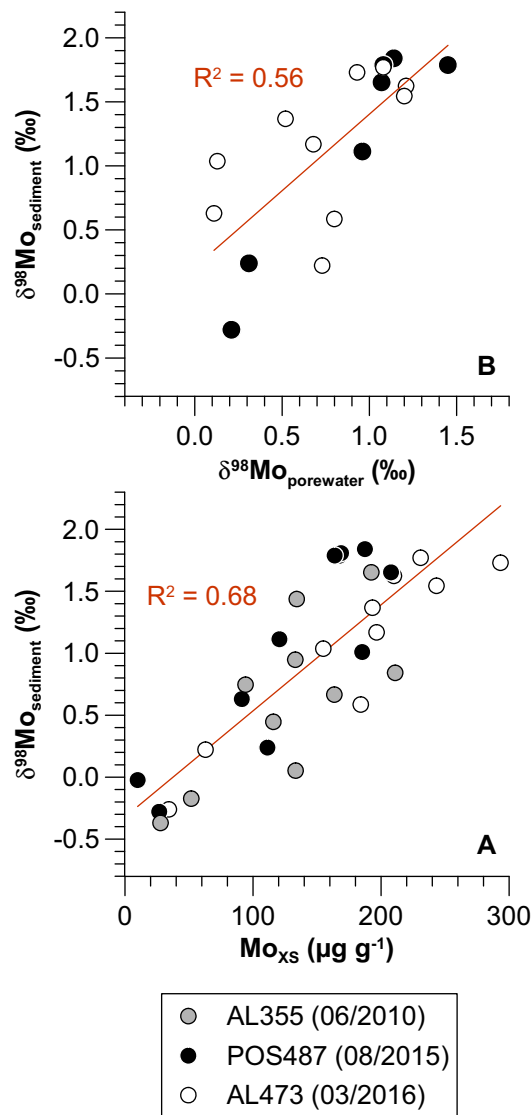


Fig. 7. Plot of (A) $\delta^{98}\text{Mo}_{\text{sediment}}$ versus Mo_{xs} and (B) $\delta^{98}\text{Mo}_{\text{pore water}}$ versus $\delta^{98}\text{Mo}_{\text{sediment}}$ for sediment cores taken before (AL355) and after (POS487, AL473) inflow.

of $+2.8\text{‰}$ (Siebert et al., 2003; Barling and Anbar, 2004; Wasylenko et al., 2008) is expressed. The light $\delta^{98}\text{Mo}_{\text{sediment}}$ values observed in the Gotland Deep prior to the onset of anoxia around the turn of the 20th century are likely due to a similar mode of sedimentary Mo uptake under oxic and Mo replete conditions. The shift to slightly heavier $\delta^{98}\text{Mo}$ values in the Gotland Deep compared to the deep Pacific Ocean could be related to a higher proportion of Mo delivered by Fe (oxyhydr)oxides which is known to carry a heavier Mo isotope composition than Mo adsorbed to Mn (oxyhydr)oxides (Goldberg et al., 2009).

The increase in TOC and Mo concentrations above 20 cm sediment depth is accompanied by a transition to heavier $\delta^{98}\text{Mo}_{\text{sediment}}$ values ($+1.23 \pm 0.50\text{‰}$, 1 SD, $n = 25$) (Fig. 5). Overall, $\delta^{98}\text{Mo}_{\text{sediment}}$

Table 3
Diffusive flux calculations.

Cruise	Station	Device	Water depth (m)	Temperature (°C)	Salinity	Porosity	D_{sed}^a ($\text{cm}^2 \text{s}^{-1}$)	$d[\text{Mo}]/dx$ ($\text{nmol cm}^{-3} \text{cm}^{-1}$)	F_{Mo} ($\mu\text{mol m}^{-2} \text{yr}^{-1}$)
POS487	444	MUC20	228	6.9	12.3	0.99	$5.61\text{E-}06$	−6480	$1.14\text{E} + 04$
AL473	130	MUC12	219	7.6	12.1	0.99	$5.75\text{E-}06$	−6540	$1.17\text{E} + 04$

^a Corrected for temperature, salinity, pressure and tortuosity.

displays a close correlation with Mo_{XS} concentrations (Fig. 7A). A linear regression through the data would intersect with the $\delta^{98}\text{Mo}$ of global seawater (+2.3‰) at high sedimentary Mo_{XS} concentrations of about $300 \mu\text{g g}^{-1}$. This correlation trend suggests that the intensification of hypoxia over the course of the 20th century was accompanied by increasing Mo removal from the water column with relatively little isotope fractionation relative to the Mo isotope composition of global seawater. Scavenging of MoS_4^{2-} under strictly euxinic conditions would be an obvious process which could explain this trend towards heavier $\delta^{98}\text{Mo}_{\text{sediment}}$. Consistent with such a scenario, aqueous H_2S concentrations typically exceed the threshold value for the complete conversion of MoO_4^{2-} to MoS_4^{2-} of $11 \mu\text{M}$ during multiannual euxinic periods (e.g., Neretin et al., 2003; Meyer et al., 2012; Scholz et al., 2013). At the same time, our flux calculations clearly show that a significant fraction of the sedimentary Mo is supplied by Mn (oxyhydr)oxides deposited during oxygenation events (see Section 4.3). Consistent with this notion, the shallow peak in dissolved (Fig. 5) and particulate (Fig. 4) Mn in the sediment core from AL473 is accompanied by a relatively light $\delta^{98}\text{Mo}_{\text{porewater}}$ (+0.11‰) (Note that the uppermost 2 to 3 cm of sediment of the other post-inflow core from POS487 were lost during core recovery). The addition of this isotopically light Mo from Mn (oxyhydr)oxide dissolution to preexisting organic matter is likely reflected by the relatively broad range of $\delta^{98}\text{Mo}_{\text{sediment}}$ observed in the concentration range between 100 and $200 \mu\text{g g}^{-1}$ (up to 1.5‰ at similar Mo_{XS}) (Fig. 7A). To quantify the Mo fractions delivered during euxinic periods and oxygenation events, we assume that the sedimentary Mo_{XS} and Mo isotope pool is generated by two-component mixing which can be expressed with the following equation:

$$\delta^{98}\text{Mo}_{\text{sediment}} = f \cdot \delta^{98}\text{Mo}_{\text{euxinic}} + (1 - f) \cdot \delta^{98}\text{Mo}_{\text{oxygenation}} \quad (6)$$

Although it is possible that some of the sedimentary Mo was delivered during periods with weakly sulfidic conditions (i.e., when partial conversion of MoO_4^{2-} to MoS_4^{2-} or intermediate thiomolybdate imparts an isotope fractionation to the deposited Mo fraction (e.g., Nägler et al., 2011)), we have no means to determine the isotope composition of this likely subordinate Mo fraction. Therefore, we do not consider it in our mass balance calculations.

By re-arranging Eq. (5) and adopting the $\delta^{98}\text{Mo}$ of global seawater for $\delta^{98}\text{Mo}_{\text{euxinic}}$, the average $\delta^{98}\text{Mo}$ below 20 cm sediment depth (i.e., corresponding to a period when Mo was deposited under oxic conditions) for $\delta^{98}\text{Mo}_{\text{oxygenation}}$ ($-0.15 \pm 0.22\text{‰}$) and the $\delta^{98}\text{Mo}$ of sediments above 20 cm depth for $\delta^{98}\text{Mo}_{\text{sediment}}$ ($+1.23 \pm 0.50\text{‰}$) we estimate that between 25% and 65% of the sedimentary Mo is delivered by Mn (oxyhydr)oxides during oxygenation events. This calculation substantiates our findings from flux calculations that Mo delivered by Mn (oxyhydr)oxides during oxygenation events makes an important contribution to Mo burial in the Gotland Deep.

At the very sediment surface, Mo release from Mn (oxyhydr)oxides is reflected by a light $\delta^{98}\text{Mo}_{\text{porewater}}$. In contrast, below about 1 cm sediment depth, dissolved Mo in pore water is not characterized by a light isotope composition (Fig. 5). Instead, $\delta^{98}\text{Mo}_{\text{porewater}}$ generally follows $\delta^{98}\text{Mo}_{\text{sediment}}$ (Fig. 7B). Since the $\delta^{98}\text{Mo}_{\text{porewater}}$ encountered at the time of sampling does not correlate with dissolved Mo concentrations ($R^2 < 0.01$) (Fig. 5), we infer that it does not represent the isotope composition of the Mo originally delivered by Mn (oxyhydr)oxides. Instead, the covariation between $\delta^{98}\text{Mo}_{\text{porewater}}$ and $\delta^{98}\text{Mo}_{\text{sediment}}$ suggests that pore water Mo is affected by isotopic exchange with the adjacent solid phase. Because pore water Mo represents only a subordinate fraction of the total Mo (i.e., the sum of solid phase and dissolved) that is present in each depth interval (7% at most in highly porous surface sediments, generally $< 1\%$), isotopic exchange would have a strong impact on $\delta^{98}\text{Mo}_{\text{porewater}}$ but is negligible for $\delta^{98}\text{Mo}_{\text{sediment}}$. Further research on the processes that govern the isotope composition of pore water Mo is required to substantiate this hypothesis. Importantly, however, Mo removal onto preexisting organic matter

seems to enrich the pore water in the heavier Mo isotopes compared to the Mo originally delivered by Mn (oxyhydr)oxides. Part of this Mo is likely recycled into the bottom water through diffusion along the upward concentration gradient in the surface sediment (Fig. 6). This recycled Mo would further contribute to the relatively high $\delta^{98}\text{Mo}$ observed in the deep water of the Gotland Deep by Nägler et al. (2011) ($\delta^{98}\text{Mo}$ of up to +2.66‰). Considering this shift to higher $\delta^{98}\text{Mo}_{\text{euxinic}}$ in Eq. (5) would result in a further increase in the proportion of Mo delivered during oxygenation events.

5. Summary and implications for the use of molybdenum as a paleo-redox proxy

Sediment cores taken in the intermittently euxinic Gotland Deep during a series of seawater inflow and oxygenation events reveal pronounced peaks of pore water Mo in the surface sediment. These peaks are attributed to Mo release from dissolving Mn (oxyhydr)oxides which had precipitated in the water column during inflow of oxygenated seawater. Deeper in the sediment, dissolved Mo is removed from the pore water through interaction with hydrogen sulfide and organic matter. The diffusive Mo flux along the downward concentration gradient in the pore water drives Mo accumulation in the sediment. Diffusive flux calculations and a mass balance approach, which is based on the Mo isotope composition of the sediment, suggest that Mo accumulation during short-lived inflow events makes an important contribution to sedimentary Mo burial in the Gotland Deep. The sediment horizons of Mo release into and removal from the pore water are separated by several centimeters and the distance between these layers is likely to fluctuate over time as a function of the rate of Mo release and the upward H_2S flux. Therefore, the high-resolution record of Mo concentration and isotope composition in the sediment would be misinterpreted if steady state accumulation of Mo was assumed. The solid phase Mo isotope record is further complicated by apparent isotopic exchange between the solid phase and dissolved Mo pools in the sediment.

Recent water column and pore water studies in the context of both restricted euxinic basins and open-marine anoxia highlight the role of Mn and/or Fe (oxyhydr)oxides precipitating along water column redox interfaces as carrier phases for Mo to the sediment surface (e.g., Scholz et al., 2017; Ho et al., 2018). Upon dissolution of the solid carrier phases in the surface sediment, a fraction of the Mo is lost through diffusion across the sediment-water interface whereas another fraction is scavenged from the pore water in the sulfidic zone of the sediment. We argue that the balance between particulate Mo delivery, recycling and burial exerts primary control on the Mo isotope composition that is eventually recorded in the sediment. Shifts in this balance, e.g., due to changes in bottom water redox conditions on different timescales need to be considered in the interpretation of the paleo-record.

Supplementary data to this article can be found online at <https://doi.org/10.1016/j.chemgeo.2018.04.031>.

Acknowledgements

We would like to thank the crews of RV Alkor and RV Poseidon as well as our colleagues Antje Beck, Anke Bleyer, Bettina Domeyer, Asmus Petersen, Gabriele Schüssler and Regina Surberg for supporting us during sample collection and laboratory work. This study was supported by the German Research Foundation (DFG) through the Emmy Noether Nachwuchsgruppe ICONOX (“Iron Cycling in Marine Sediments and the Nutrient and Oxygen Balance of the Ocean”) to FS and Sonderforschungsbereich 754 (“Climate-Biogeochemistry Interactions in the Tropical Ocean”). Constructive comments from Stefan Weyer and an anonymous reviewer are gratefully acknowledged.

References

- Algeo, T.J., 2004. Can marine anoxic events draw down the trace element inventory of seawater? *Geology* 32, 1057–1060.
- Algeo, T.J., Lyons, T.W., 2006. Mo-total organic carbon covariation in modern anoxic marine environments: implications for analysis of paleoredox and paleohydrographic conditions. *Paleoceanography* 21, PA1016.
- Algeo, T.J., Tribouillard, N., 2009. Environmental analysis of paleoceanographic systems based on molybdenum-uranium covariation. *Chem. Geol.* 268, 211–225.
- Archer, C., Vance, D., 2008. The isotopic signature of the global riverine molybdenum flux and anoxia in the ancient oceans. *Nat. Geosci.* 1, 597–600.
- Arnold, G.L., Anbar, A.D., Barling, J., Lyons, T.W., 2004. Molybdenum isotope evidence for widespread anoxia in mid-proterozoic oceans. *Science* 304, 87–90.
- Barling, J., Anbar, A.D., 2004. Molybdenum isotope fractionation during adsorption by manganese oxides. *Earth Planet. Sci. Lett.* 217, 315–329.
- Barling, J., Arnold, G.L., Anbar, A.D., 2001. Natural mass-dependent variations in the isotopic composition of molybdenum. *Earth Planet. Sci. Lett.* 193, 447–457.
- Berelson, W., McManus, J., Coale, K., Johnson, K., Burdige, D., Kilgore, T., Colodner, D., Chavez, F., Kudela, R., Boucher, J., 2003. A time series of benthic flux measurements from Monterey Bay, CA. *Cont. Shelf Res.* 23, 457–481.
- Berrang, P.G., Grill, E.V., 1974. The effect of manganese oxide scavenging on molybdenum in saanich inlet, British Columbia. *Mar. Chem.* 2, 125–148.
- Boesen, C., Postma, D., 1988. Pyrite formation in anoxic environments of the Baltic. *Am. J. Sci.* 288, 575–603.
- Boudreau, B.P., 1996. The diffusive tortuosity of fine-grained un lithified sediments. *Geochim. Cosmochim. Acta* 60, 3139–3142.
- Bruland, K.W., 1983. Trace elements in sea-water. In: Riley, J.P., Chester, R. (Eds.), *Chemical Oceanography*. Academic Press, London, pp. 157–220.
- Brumsack, H.-J., 2006. The trace metal content of recent organic carbon-rich sediments: implications for cretaceous black shale formation. *Palaeogeogr. Palaeoclimatol. Palaeoecol.* 232, 344–361.
- Calvert, S.E., Pedersen, T.F., 1993. Geochemistry of recent oxic and anoxic marine-sediments - implications for the geological record. *Mar. Geol.* 113, 67–88.
- Calvert, S.E., Pedersen, T.F., 1996. Sedimentary geochemistry of manganese: implications for the environment of formation of manganiferous black shales. *Econ. Geol. Bull. Soc. Econ. Geol.* 91, 36–47.
- Conley, D.J., Humborg, C., Rahm, L., Savchuk, O.P., Wulff, F., 2002. Hypoxia in the Baltic Sea and basin-scale changes in phosphorus biogeochemistry. *Environ. Sci. Technol.* 36, 5315–5320.
- Conley, D.J., Björck, S., Bonsdorff, E., Carstensen, J., Destouni, G., Gustafsson, B.G., Hietanen, S., Kortekaas, M., Kuosa, H., Markus Meier, H.E., Müller-Karulis, B., Nordberg, K., Norrko, A., Nürnberg, G., Pitkänen, H., Rabalais, N.N., Rosenberg, R., Savchuk, O.P., Slomp, C.P., Voss, M., Wulff, F., Zillén, L., 2009. Hypoxia-related processes in the Baltic Sea. *Environ. Sci. Technol.* 43, 3412–3420.
- Dahl, T.W., Anbar, A.D., Gordon, G.W., Rosing, M.T., Frei, R., Canfield, D.E., 2010. The behavior of molybdenum and its isotopes across the chemocline and in the sediments of sulfidic Lake Cadagno, Switzerland. *Geochim. Cosmochim. Acta* 74 (1), 144–163.
- Dahl, T.W., Chappaz, A., Fitts, J.P., Lyons, T.W., 2013. Molybdenum reduction in a sulfidic lake: evidence from X-ray absorption fine-structure spectroscopy and implications for the Mo paleoproxy. *Geochim. Cosmochim. Acta* 103, 213–231.
- Dahl, T.W., Chappaz, A., Hoek, J., McKenzie, C.J., Svane, S., Canfield, D.E., 2017. Evidence of molybdenum association with particulate organic matter under sulfidic conditions. *Geobiology* 15, 311–323.
- Dale, A.W., Graco, M., Wallmann, K., 2017. Strong and dynamic benthic-pelagic coupling and feedbacks in a coastal upwelling system (Peruvian shelf). *Front. Mar. Sci.* 4. <http://dx.doi.org/10.3389/fmars.2017.00029>.
- Dellwig, O., Leipe, T., März, C., Glockzin, M., Pollehn, F., Schmetzer, B., Yakushev, E.V., Böttcher, M.E., Brumsack, H.-J., 2010. A new particulate Mn-Fe-P-shuttle at the redoxcline of anoxic basins. *Geochim. Cosmochim. Acta* 74, 7100–7115.
- Dickson, A.J., 2017. A molybdenum-isotope perspective on Phanerozoic deoxygenation events. *Nat. Geosci.* 10, 721–726.
- Dyrssen, D., Kremling, K., 1990. Increasing hydrogen sulfide concentration and trace metal behavior in the anoxic Baltic waters. *Mar. Chem.* 30, 193–204.
- Erickson, B.E., Helz, G.R., 2000. Molybdenum(VI) speciation in sulfidic waters: stability and lability of thiomolybdates. *Geochim. Cosmochim. Acta* 64, 1149–1158.
- Fehr, M.A., Andersson, P.S., Hålenius, U., Möhr, C.-M., 2008. Iron isotope variations in Holocene sediments of the Gotland deep, Baltic Sea. *Geochim. Cosmochim. Acta* 72, 807–826.
- Fehr, M.A., Andersson, P.S., Hålenius, U., Gustafsson, Ö., Möhr, C.-M., 2010. Iron enrichments and Fe isotopic compositions of surface sediments from the Gotland deep, Baltic Sea. *Chem. Geol.* 277, 310–322.
- Feistel, R., Nausch, G., Hagen, E., 2006. Unusual Baltic inflow activity in 2002–2003 and varying deep-water properties. *Oceanologia* 48, 21–35.
- Goldberg, T., Archer, C., Vance, D., Poulton, S.W., 2009. Mo isotope fractionation during adsorption to Fe (oxyhydr)oxides. *Geochim. Cosmochim. Acta* 73, 6502–6516.
- Goldberg, T., Archer, C., Vance, D., Thamdrup, B., Anena, A.M., Poulton, S.W., 2012. Controls on Mo isotope fractionations in a Mn-rich anoxic marine sediment, Gullmar Fjord, Sweden. *Chem. Geol.* 296–297, 73–82.
- Goldberg, T., Poulton, S.W., Wagner, T., Kolonic, S.F., Rehämper, M., 2016. Molybdenum drawdown during cretaceous oceanic anoxic event 2. *Earth Planet. Sci. Lett.* 440, 81–91.
- Grasshoff, K., Erhardt, M., Kremling, K., 2002. *Methods of Seawater Analysis*. Weinheim, Wiley VCH.
- Gräwe, U., Naumann, M., Burchard, H., Mohrholz, V., 2015. Anatomizing one of the largest saltwater inflows into the Baltic Sea in December 2014. *J. Geophys. Res.* Oceans 120, 7676–7697.
- Greber, N.D., Siebert, C., Nägler, T.F., Pettke, T., 2012. $\delta^{98/95}\text{Mo}$ values and molybdenum concentration data for NIST SRM 610, 612 and 3134: towards a common protocol for reporting Mo data. *Geostand. Geoanal. Res.* 36, 291–300.
- Hammarlund, E.U., Dahl, T.W., Harper, D.A.T., Bond, D.P.G., Nielsen, A.T., Bjerrum, C.J., Schovsbo, N.H., Schönlaub, H.P., Zalasiewicz, J.A., Canfield, D.E., 2012. A sulfidic driver for the end-Ordovician mass extinction. *Earth Planet. Sci. Lett.* 331–332, 128–139.
- Heiser, U., Neumann, T., Scholten, J., Stüben, D., 2001. Recycling of manganese from anoxic sediments in stagnant basins by seawater inflow: a study of surface sediments from the Gotland Basin, Baltic Sea. *Mar. Geol.* 177 (1–2), 151–166.
- Helz, G.R., Miller, C.V., Charnock, J.M., Mosselmans, J.F.W., Patrick, R.A.D., Garner, C.D., Vaughan, D.J., 1996. Mechanism of molybdenum removal from the sea and its concentration in black shales: EXAFS evidence. *Geochim. Cosmochim. Acta* 60, 3631–3642.
- Helz, G.R., Bura-Nakic, E., Mikac, N., Ciglenecki, I., 2011. New model for molybdenum behavior in euxinic waters. *Chem. Geol.* 284, 323–332.
- Hille, S., Leipe, T., Seifert, T., 2006. Spatial variability of recent sedimentation rates in the eastern Gotland Basin (Baltic Sea). *Oceanologia* 48, 297–317.
- Ho, P., Lee, J.-M., Heller, M.I., Lam, P.J., Shiller, A.M., 2018. The distribution of dissolved and particulate Mo and V along the U.S. GEOTRACES East Pacific zonal transect (GP16): the roles of oxides and biogenic particles in their distributions in the oxygen deficient zone and the hydrothermal plume. *Mar. Chem.* 201, 242–255.
- Huckriede, H., Meischner, D., 1996. Origin and environment of manganese-rich sediments within black-shale basins. *Geochim. Cosmochim. Acta* 60, 1399–1413.
- Huerta-Diaz, M.A., Morse, J.W., 1992. Pyritization of trace metals in anoxic marine sediments. *Geochim. Cosmochim. Acta* 56, 2681–2702.
- Jacobs, L., Emerson, S., Huested, S.S., 1987. Trace metal geochemistry in the Cariaco trench. *Deep Sea Oceanograph. Res. Papers* 34, 965–981.
- Jakobsen, R., Postma, D., 1989. Formation and solid solution behavior of Ca-rhodochrosites in marine muds of the Baltic deep. *Geochim. Cosmochim. Acta* 53, 2639–2648.
- Jilbert, T., Slomp, C.P., 2013a. Iron and manganese shuttles control the formation of authigenic phosphorus minerals in the euxinic basins of the Baltic Sea. *Geochim. Cosmochim. Acta* 107, 155–169.
- Jilbert, T., Slomp, C.P., 2013b. Rapid high-amplitude variability in Baltic Sea hypoxia during the Holocene. *Geology* 41, 1183–1186.
- Jilbert, T., Slomp, C.P., Gustafsson, B.G., Boer, W., 2011. Beyond the Fe-P-redox connection: preferential regeneration of phosphorus from organic matter as a key control on Baltic Sea nutrient cycles. *Biogeosciences* 8, 1699–1720.
- Kendall, B., Komiya, T., Lyons, T.W., Bates, S.M., Gordon, G.W., Romaniello, S.J., Jiang, G., Creaser, R.A., Xiao, S., McFadden, K., Sawaki, Y., Tahata, M., Shu, D., Han, J., Li, Y., Chu, X., Anbar, A.D., 2015. Uranium and molybdenum isotope evidence for an episode of widespread ocean oxygenation during the late Ediacaran period. *Geochim. Cosmochim. Acta* 156, 173–193.
- Leipe, T., Dippner, J.W., Hille, S., Voss, M., Christiansen, C., Bartholdy, J., 2008. Environmental changes in the Central Baltic Sea during the past 1000 years: inferences from sedimentary records, hydrography and climate. *Oceanologia* 50, 23–41.
- Lenz, C., Jilbert, T., Conley, D.J., Slomp, C.P., 2015a. Hypoxia-driven variations in iron and manganese shuttling in the Baltic Sea over the past 8 kyr. *Geochim. Geophys. Geosyst.* 16, 3754–3766.
- Lenz, C., Jilbert, T., Conley, D.J., Wolthers, M., Slomp, C.P., 2015b. Are recent changes in sediment manganese sequestration in the euxinic basins of the Baltic Sea linked to the expansion of hypoxia? *Biogeosciences* 12, 4875–4894.
- Li, Y.-H., Gregory, S., 1974. Diffusion of ions in sea water and in deep-sea sediments. *Geochim. Cosmochim. Acta* 38, 703–714.
- Lyons, T.W., Severmann, S., 2006. A critical look at iron paleoredox proxies: new insights from modern euxinic marine basins. *Geochim. Cosmochim. Acta* 70, 5698–5722.
- Matthäus, W., Franck, H., 1992. Characteristics of major Baltic inflows - a statistical analysis. *Cont. Shelf Res.* 12, 1375–1400.
- Matthäus, W., Nehring, D., Feistel, R., Nausch, G., Mohrholz, V., Lass, H.U., 2008. The inflow of highly saline water into the Baltic Sea. In: Feistel, R., Nausch, G., Wasmund, N. (Eds.), *State and Evolution of the Baltic Sea, 1952–2005. A Detailed 50-Year Survey of Meteorology and Climate, Physics, Chemistry, Biology, and Marine Environment*. John Wiley & Sons, Hoboken, pp. 265–309.
- McLennan, S.M., 2001. Relationships between the Trace Element Composition of Sedimentary Rocks and Upper Continental Crust. *Geochemistry Geophysics Geosystems* 2. In: Paper number 2000GC000109.
- McManus, J., Nägler, T.F., Siebert, C., Wheat, C.G., Hammond, D.E.C., 2002. Oceanic molybdenum isotope fractionation: Diagenesis and hydrothermal ridge-flank alteration. *sGeochem. Geophys. Geosyst.* 3. <http://dx.doi.org/10.1029/2002GC000356>.
- McManus, J., Berelson, W.M., Severmann, S., Poulson, R.L., Hammond, D.E., Klinkhammer, G.P., Holm, C., 2006. Molybdenum and uranium geochemistry in continental margin sediments: Paleoproxy potential. *Geochim. Cosmochim. Acta* 70, 4643–4662.
- Meyer, D., Prien, R.D., Dellwig, O., Connelly, D.P., Schulz-Bull, D.E., 2012. In situ determination of iron(II) in the anoxic zone of the Central Baltic Sea using ferene as spectrophotometric reagent. *Mar. Chem.* 130–131, 21–27.
- Miller, C.A., Peucker-Ehrenbrink, B., Walker, B.D., Marcantonio, F., 2011. Re-assessing the surface cycling of molybdenum and rhenium. *Geochim. Cosmochim. Acta* 75, 7146–7179.
- Mohrholz, V., Naumann, M., Nausch, G., Krüger, S., Gräwe, U., 2015. Fresh oxygen for the Baltic Sea – an exceptional saline inflow after a decade of stagnation. *J. Mar. Syst.* 148, 152–166.
- Montoya-Pino, C., Weyer, S., Anbar, A.D., Pross, J., Oschmann, W., van de Schootbrugge,

- B., Arz, H.W., 2010. Global enhancement of ocean anoxia during oceanic anoxic event 2: a quantitative approach using U isotopes. *Geology* 38, 315–318.
- Nägler, T.F., Neubert, N., Böttcher, M.E., Dellwig, O., Schnetger, B., 2011. Molybdenum isotope fractionation in pelagic euxinia: evidence from the modern black and Baltic seas. *Chem. Geol.* 289, 1–11.
- Nägler, T.F., Anbar, A.D., Archer, C., Goldberg, T., Gordon, G.W., Greber, N.D., Siebert, C., Sohrin, Y., Vance, D., 2014. Proposal for an international molybdenum isotope measurement standard and data representation. *Geostand. Geoanal. Res.* 38, 149–151.
- Naumann, M., Mohrholz, V., Waniek, J.J., 2017. Water exchange between the Baltic Sea and the North Sea, and conditions in the deep basins. In: *HELCOM Baltic Sea Environmental Fact Sheet Online*, <http://www.helcom.fi/baltic-sea-trends/environment-fact-sheets/>.
- Neretin, L.N., Pohl, C., Jost, G.N., Leipe, T., Pollehne, F., 2003. Manganese cycling in the Gotland deep, Baltic Sea. *Mar. Chem.* 82, 125–143.
- Neubert, N., Nägler, T.F., Böttcher, M.E., 2008. Sulfidity controls molybdenum isotope fractionation into euxinic sediments: evidence from the modern Black Sea. *Geology* 36, 775–778.
- Neumann, T., Christiansen, C., Clasen, S., Emeis, K.C., Kunzendorf, H., 1997. Geochemical records of salt-water inflows into the deep basins of the Baltic Sea. *Cont. Shelf Res.* 17, 95–115.
- Neumann, T., Heiser, U., Leosson, M.A., Kersten, M., 2002. Early diagenetic processes during Mn-carbonate formation: evidence from the isotopic composition of authigenic Ca-rhodochrosites of the Baltic Sea. *Geochim. Cosmochim. Acta* 66, 867–879.
- Noffke, A., Sommer, S., Dale, A.W., Hall, P.O.J., Pfannkuche, O., 2016. Benthic nutrient fluxes in the eastern Gotland Basin (Baltic Sea) with particular focus on microbial mat ecosystems. *J. Mar. Syst.* 158, 1–12.
- Noordmann, J., Weyer, S., Montoya-Pino, C., Dellwig, O., Neubert, N., Eckert, S., Paetzel, M., Böttcher, M.E., 2015. Uranium and molybdenum isotope systematics in modern euxinic basins: case studies from the Central Baltic Sea and the Kyllaren fjord (Norway). *Chem. Geol.* 396, 182–195.
- Pohl, C., Fernández-Otero, E., 2012. Iron distribution and speciation in oxic and anoxic waters of the Baltic Sea. *Mar. Chem.* 145–147, 1–15.
- Poulson Brucker, R.L., McManus, J., Severmann, S., Berelson, W.M., 2009. Molybdenum behavior during early diagenesis: insights from Mo isotopes. *Geochem. Geophys. Geosyst.* 10 Q06010. <https://doi.org/10.1029/2008GC002180>.
- Poulton, S.W., Fralick, P.W., Canfield, D.E., 2010. Spatial variability in oceanic redox structure 1.8 billion years ago. *Nat. Geosci.* 3, 486–490.
- Raiswell, R., Anderson, T.F., 2005. Reactive iron enrichment in sediments deposited beneath euxinic bottom waters: constraints on supply by shelf recycling. *Geol. Soc. Lond., Spec. Publ.* 248, 179–194.
- Reissmann, J.H., Burchard, H., Feistel, R., Hagen, E., Lass, H.U., Mohrholz, V., Nausch, G., Umlauf, L., Wiczeorek, G., 2009. Vertical mixing in the Baltic Sea and consequences for eutrophication - a review. *Prog. Oceanogr.* 82, 47–80.
- Schinke, H., Matthäus, W., 1998. On the causes of major Baltic inflows - an analysis of long time series. *Cont. Shelf Res.* 18, 67–97.
- Scholz, F., Hensen, C., Noffke, A., Rohde, A., Liebetrau, V., Wallmann, K., 2011. Early diagenesis of redox-sensitive trace metals in the Peru upwelling area: response to ENSO-related oxygen fluctuations in the water column. *Geochim. Cosmochim. Acta* 75, 7257–7276.
- Scholz, F., McManus, J., Sommer, S., 2013. The manganese and iron shuttle in a modern euxinic basin and implications for molybdenum cycling at euxinic ocean margins. *Chem. Geol.* 355, 56–68.
- Scholz, F., Siebert, C., Dale, A.W., Frank, M., 2017. Intense molybdenum accumulation in sediments underneath a nitrogenous water column and implications for the reconstruction of paleo-redox conditions based on molybdenum isotopes. *Geochim. Cosmochim. Acta* 213, 400–417.
- Scott, C., Lyons, T.W., 2012. Contrasting molybdenum cycling and isotopic properties in euxinic versus non-euxinic sediments and sedimentary rocks: refining the paleoproxies. *Chem. Geol.* 324–325, 19–27.
- Seifert, T., Tauber, F., Kayser, B., 2001. A High Resolution Spherical Grid Topography of the Baltic Sea, 2nd ed. Baltic Sea Science Congress, Stockholm, pp. 25–29 (November 2001, Poster #147).
- Shaw, T.J., Gieskes, J.M., Jahnke, R.A., 1990. Early diagenesis in differing depositional environments: the response of transition metals in pore water. *Geochim. Cosmochim. Acta* 54, 1233–1246.
- Siebert, C., Nägler, T.F., Kramers, J.D.C., 2001. Determination of molybdenum isotope fractionation by double-spike multicollector inductively coupled plasma mass spectrometry. *Geochem. Geophys. Geosyst.* 2. <http://dx.doi.org/10.1029/2000GC000124>.
- Siebert, C., Nägler, T.F., von Blanckenburg, F., Kramers, J.D., 2003. Molybdenum isotope records as a potential new proxy for paleoceanography. *Earth Planet. Sci. Lett.* 211, 159–171.
- Sommer, S., Clemens, D., Yücel, M., Pfannkuche, O., Hall, P.O.J., Almröth-Rosell, E., Schulz-Vogt, H.N., Dale, A.W., 2017. Major bottom water ventilation events do not significantly Reduce Basin-wide benthic N and P release in the eastern Gotland Basin (Baltic Sea). *Front. Mar. Sci.* 4. <http://dx.doi.org/10.3389/fmars.2017.00018>.
- Sternbeck, J., Sohlenius, G., 1997. Authigenic sulfide and carbonate mineral formation in Holocene sediments of the Baltic Sea. *Chem. Geol.* 135, 55–73.
- Suess, E., 1979. Mineral phases formed in anoxic sediments by microbial decomposition of organic matter. *Geochim. Cosmochim. Acta* 43, 339–352.
- Tossell, J.A., 2005. Calculating the partitioning of the isotopes of Mo between oxidic and sulfidic species in aqueous solution. *Geochim. Cosmochim. Acta* 69, 2981–2993.
- Tribouillard, N., Riboulleau, A., Lyons, T., Baudin, F., 2004. Enhanced trapping of molybdenum by sulfurized marine organic matter of marine origin in Mesozoic limestones and shales. *Chem. Geol.* 213, 385–401.
- Tribouillard, N., Algeo, T.J., Lyons, T.W., Riboulleau, A., 2006. Trace metals as paleo-redox and paleoproductivity proxies: an update. *Chem. Geol.* 232, 12–32.
- Ulfbo, A., Hulth, S., Anderson, L.G., 2011. pH and biogeochemical processes in the Gotland Basin of the Baltic Sea. *Mar. Chem.* 127, 20–30.
- Vorlíček, T.P., Helz, G.R., 2002. Catalysis by mineral surfaces: implications for Mo geochemistry in anoxic environments. *Geochim. Cosmochim. Acta* 66 (21), 3679–3692.
- Vorlíček, T.P., Kahn, M.D., Kasuya, Y., Helz, G.R., 2004. Capture of molybdenum in pyrite-forming sediments: role of ligand-induced reduction by polysulfides. *Geochim. Cosmochim. Acta* 68, 547–556.
- Wagner, M., Chappaz, A., Lyons, T.W., 2017. Molybdenum speciation and burial pathway in weakly sulfidic environments: insights from XAFS. *Geochim. Cosmochim. Acta* 206, 18–29.
- Wasylenki, L.E., Rolfe, B.A., Weeks, C.L., Spiro, T.G., Anbar, A.D., 2008. Experimental investigation of the effects of temperature and ionic strength on Mo isotope fractionation during adsorption to manganese oxides. *Geochim. Cosmochim. Acta* 72, 5997–6005.
- Westermann, S., Vance, D., Cameron, V., Archer, C., Robinson, S.A., 2014. Heterogeneous oxygenation states in the Atlantic and Tethys oceans during oceanic anoxic event 2. *Earth Planet. Sci. Lett.* 404, 178–189.
- Wille, M., Nägler, T.F., Lehmann, B., Schroder, S., Kramers, J.D., 2008. Hydrogen sulphide release to surface waters at the Precambrian/Cambrian boundary. *Nature* 453, 767–769.
- Zheng, Y., Anderson, R.F., van Geen, A., Kuwabara, J., 2000. Authigenic molybdenum formation in marine sediments: a link to pore water sulfide in the Santa Barbara Basin. *Geochim. Cosmochim. Acta* 64, 4165–4178.
- Zillén, L., Conley, D.J., Andrén, T., Andrén, E., Björck, S., 2008. Past occurrences of hypoxia in the Baltic Sea and the role of climate variability, environmental change and human impact. *Earth Sci. Rev.* 91, 77–92.